Journal of the Korean Society of Marine Environment & Safety
Vol. 18, No. 3, 2012. 6. 30., pp. 199-205 (ISSN 1229-3431)

Damping of Water Waves over Permeable Bed of Finite Depth

Gun-Woo Kim* · Myung-Eun Lee**†

* Department of Ocean Civil & Plant Construction Engineering, Mokpo National Maritime University, Mokpo, 530-729, Republic of Korea
** Department of Civil and Environmental Engineering, Seoul National University, Seoul, 151-742, Republic of Korea

유한한 깊이의 투수층에 의한 파랑의 감쇠

김건우* · 이명은**†

* 목포해양대학교, ** 서울대학교

Abstract : *In this study, wave transformation by damping due to the permeable bed of finite depth is investigated. The relationship between wave damping rate and relative water depth are presented. The damping rate is used in the eigenfunction expansion method to calculate the wave dissipation over the permeable bed. For a permeable shoal, the eigenfunction expansion model result is compared with that of the integral equation method to show good agreement. The model is also used to examine the wave reflection over the permeable planar slope of various frequency. It has been found that in general relatively short waves are more influenced by the permeability of the permeable seabed than relatively long waves unless the water depth is so large that the influence of permeable bed on surface water waves disappears.*

Key Words : *Eigenfunction expansion method, Wave damping, Permeable seabed, Wave scattering, Monochromatic wave*

요 약 : 본 연구에서는 유한한 깊이의 투수층에 의한 에너지 감쇠효과를 고려한 파랑의 변형을 해석하였다. 파의 에너지 감쇠율과 상대수심의 관계식을 제시하였으며, 에너지 감쇠율을 고유함수전개법에 사용하여 투수층에 의한 에너지 감쇠를 계산하였다. 투수성이 있는 수중둔덕에 대해서, 수치실험 결과는 해석해로 간주할 수 있는 적분방정식의 결과와 비교하여 잘 일치하였다. 또한, 투수경사에 의한 반사율을 다양한 주파수에 대해서 실험하였으며, 수치실험 결과, 수심이 매우 커서 수면파가 투수층의 영향을 받을 정도가 아닌 경우에는 상대적으로 파장이 짧은 파랑일수록 투수층의 영향을 크게 받는 것으로 나타났다.

핵심용어 : 고유함수전개법, 파랑 감쇠, 투수성 바닥, 파랑 산란, 선형파

1. Introduction

As wind waves generated in deep water approach the nearshore zone, they experience many important physical phenomena caused by bathymetric variations, nonlinear interactions among different wave components and interferences with coastal structures. Among these, the bathymetric variations play a significant role in the change of the wave transformation. Thus, harbor engineers should have a proper tool for estimating the wave climate as accurately as possible to design a coastal structure in nearshore area.

The propagation of monochromatic surface waves over a variational bathymetry has been investigated through theoretical, experimental and numerical studies because of its practical application in designing of submerged coastal structures. In order to solve the case of normal wave incidence and arbitrary relative depth over a sill or a fixed obstacle at the surface, Takano(1960) employed an eigenfunction expansion of the velocity potentials in each constant depth region and matched them at the region boundaries. The set of linear integral equation was solved for a truncated series. The problem of obliquely incident waves over an asymmetric trench was solved by Kirby and Dalrymple(1983) using a modified form of Takano's method. O'Hare and Davies(1992) and Guazzelli et al.(1992) presented a new method for the modeling of propagation of monochromatic waves over a smoothly varying bottom topography by dividing the topography into a series of small steps and calculated the reflection and transmission coefficient by using scattering matrix method. The previous studies have all

* First author : gwkim@mmu.ac.kr, 061-240-7319
† Corresponding author : lmeun88@snu.ac.kr, 010-2515-2871

investigated the interaction of water waves with changes in impermeable bathymetry.

Viscous damping of nearshore waves over a permeable seabed has long been recognized as an important coastal engineering problem. Reid and Kajiura(1957) derived the damping rate of waves traveling over an infinitely deep permeable seabed on the assumption that the flow inside the bed is governed by the Darcy's equation. Later, Liu and Dalrymple(1984) derived the wave damping rate over a permeable seabed of finite depth by expressing the flow inside the bed by the generalized Darcy's equation, which considers additional wave damping inside the boundary layers between water and soil and between soil and impermeable stratum. However, they found that the damping is largely due to the energy losses in the porous medium rather than the boundary layer losses. Recently, Do and Suh(2011) derived the wave damping rate for the wave propagating over a multi-layered permeable seabed of finite depth.

In this study, we develop a theoretical model based on the eigenfunction expansion method to simulate the propagation of monochromatic waves over an porous bathymetry. We extended the eigenfunction expansion method by including the wave damping rate of waves propagating over a permeable seabed of finite depth. Numerical experiments are conducted for a permeable sea bed and permeable planar slope with several wave frequencies.

2. Derivation of wave damping rate

We consider the waves propagating over a permeable seabed of finite depth as presented in Fig. 1, in which h is the water depth, and d is the width of the permeable bed. Ω_1 and Ω_2 indicate the fluid region and permeable bed region, respectively. Hereinafter, the numeric subscripts indicate the variables in these regions.

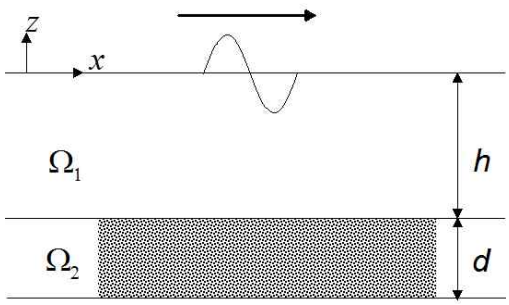

Fig. 1. Definition sketch of permeable seabed of finite depth.

In the fluid, the Laplace equation with respect to the velocity potential ϕ_1 and the linearized free surface boundary conditions must be satisfied:

$$\nabla^2\phi_1 = 0 \tag{1}$$

$$\frac{\partial\phi_1}{\partial t} = g\eta \quad \text{at} \quad z = 0 \tag{2}$$

$$\frac{\partial\eta}{\partial t} = \frac{\partial\phi_1}{\partial z} \quad \text{at} \quad z = 0 \tag{3}$$

where $\nabla = \boldsymbol{i}\partial/\partial x + \boldsymbol{k}\partial/\partial z$ with $\boldsymbol{i}$ and $\boldsymbol{k}$ being unit vectors in x and z directions, respectively, g gravitational acceleration, and η is the free surface elevation.

For a fully saturated soil in Ω_2, which is assumed to be incompressible, the continuity equation is:

$$\nabla \cdot \boldsymbol{u}_2 = 0 \tag{4}$$

where $\boldsymbol{u}_2$ is the velocity in the porous layer. The Darcy's law relates the velocity to the pressure gradient by

$$\boldsymbol{u}_2 = -\frac{K}{\mu}\nabla p_2 \tag{5}$$

where K is the permeability, μ the dynamic viscosity of the fluid, and p_2 is the pressure inside the porous layer. substituting Eq. (5) into Eq. (4) leads to

$$\nabla^2 p_2 = 0 \tag{6}$$

Thus the pore pressure also satisfies the Laplace equation. The velocity potential ϕ_1 and pore pressure p_2 can be assumed to be

$$\phi_1(x,z) = [A\cosh k(h+z) + B\sinh k(h+z)]e^{i(kx-\sigma t)} \tag{7}$$

$$p_1(x,t) = [C\cosh k(h+z+d) + D\sinh k(h+z+d)]e^{i(kx-\sigma t)} \tag{8}$$

where k is the wave number, σ is the wave angular frequency, and $i = \sqrt{-1}$. These solutions satisfy the Laplace equations for ϕ_1 and p_2. The unknown coefficients A to D and the dispersion relationship can be obtained by using the boundary conditions at the free surface and impermeable stratum and the matching conditions at the interface between fluid and soil.

First, the bottom boundary condition is expressed as

$$w_2 = 0 \qquad \text{at } z = -h-d \tag{9}$$

The continuity of pressure and vertical velocity across the interface between fluid and soil requires that

$$\rho\frac{\partial\phi_1}{\partial t} = p_2 \qquad \text{at } z = -h \tag{10}$$

$$-\frac{\partial\phi_1}{\partial z} = -\frac{K}{\mu}\frac{\partial p_2}{\partial z} \qquad \text{at } z = -h \tag{11}$$

using the boundary condition at the impermeable stratum:

$$\frac{\partial p_2}{\partial z} = 0 \text{ at } z = -h-d \tag{12}$$

Applying these matching conditions along with the surface boundary conditions to Eqs. (7) and (8) yields the coefficients A to D and the dispersion relationship as

$$\sigma^2 - gk\tanh kh = -i\frac{\sigma K}{\nu}(gk - \sigma^2\tanh kh)\tanh kd \tag{13}$$

where ν is the kinematic viscosity of the fluid. This dispersion relationship is complex, yielding a complex k, which may be written as

$$k = k^r + ik^i \tag{14}$$

The real part of k represents the real wave number related to the wavelength, while the imaginary part determines the spatial damping rate. In intermediate depth and shallow water, the real and imaginary parts yield

$$\sigma^2 = gk^r\tanh(k^r h) \tag{15}$$

$$k^i = \frac{\sigma K}{\nu}\frac{2k^r}{2k^r h + \sinh(2k^r h)}\tanh(k^r d) \tag{16}$$

If the depth of the permeable bed is very large, Eq. (16) reduces to the wave damping rate of Reid and Kajiura(1957) for an infinitely deep permeable bed.

3. Eigenfunction expansion method

The two-dimensional motion of monochromatic, small amplitude water waves in an inviscid and irrotational fluid of arbitrary depth over a permeable bed of finite depth is investigated. The waves are normally incident and propagate in an infinitely long channel containing a two-dimensional variable depth of finite width.

The eigenfunction expansion method is an extension of the Takano(1960) formulation for the propagation of waves over a rectangular sill. In the present formulation, we extended the eigenfunction expansion method including the dissipating effect by the porous bed of finite depth.

The solution starts with the definition of a velocity potential:

$$\widetilde{\phi}_j(x,z,t) = \phi_j(x,z)\exp(i\sigma t) \qquad j = 1,\cdots,J \tag{17}$$

where j indicates the region, J is the wave number of region, and σ is the angular frequency. The velocity potential should satisfy the Laplace equation:

$$\left(\frac{\partial^2}{\partial x^2} + \frac{\partial^2}{\partial z^2}\right)\phi(x,z) = 0 \tag{18}$$

The free-surface boundary condition is:

$$\frac{\partial\phi(x,z)}{\partial z} + \frac{\sigma^2}{g}\phi(x,z) = 0 \qquad \text{at } z = 0 \tag{19}$$

The condition of no flow normal to any solid boundary is:

$$\frac{\partial\phi(x,z)}{\partial \boldsymbol{n}} = 0 \tag{20}$$

where $\boldsymbol{n}$ denotes the unity vector pointing into the fluid domain, normal to the boundary defined by water depth. The velocity potentials for the scattered waves must satisfy the radiation condition.

The boundary value problem defined by Eq. (18), the boundary conditions of Eqs. (19) and (20), and the radiation condition can be solved with a solution in each region of the form:

$$\begin{aligned}\phi_j(x,z) = {} & A_j^{\pm}\cosh[k_j^r(h_j+z)]e^{\pm i(k_j^r x + ik_j^i x)} \\ & + \sum_{n=1}^{\infty} B_{j,n}^{\pm}\cos[\kappa_{j,n}(h_j+z)]e^{\pm\kappa_{j,n}(x-x_j)}\end{aligned} \tag{21}$$

where superscripts + and − denote the right-going and the left-going wave components, respectively. In the above equation, A_1^+ is the incident wave amplitude coefficient, A_1^-

is the reflected wave amplitude coefficient, and A_j^+ is the transmitted wave amplitude coefficient. The coefficient B is an amplitude function for the evanescent modes at the boundaries, which are standing waves that decay exponentially with distance from the boundary. The values of the wave number for the propagating modes, k_j^r, are determined from the dispersion relation:

$$\sigma^2 = gk_j^r \tanh(k_j^r h_j) \qquad j=1,\cdots,J \tag{22}$$

and the wave numbers for the evanescent modes, $\kappa_{j,n}$ are found from:

$$\sigma^2 = g\kappa_{j,n} \tan(\kappa_{j,n} h_j) \qquad j=1,\cdots,J,\ n=1,\cdots,\infty \tag{23}$$

The values of the damping rate, k_j^i can be obtained from Eq. (16). In each region, a complete set of orthogonal equations over the depth is formed by Eqs. (21) - (23).

To gain the full solution, matching conditions are applied at each boundary between adjacent regions. In the absence of a current, the matching conditions ensuring continuity of pressure are:

$$\phi_j = \phi_{j+1} \qquad \text{at } x = x_j \tag{24}$$

and continuity of horizontal velocity normal to the vertical boundaries:

$$\frac{\partial \phi_j}{\partial x} = \frac{\partial \phi_{j+1}}{\partial x} \qquad \text{at } x = x_j \tag{25}$$

The matching conditions are applied over the vertical plane between the two region:

In the step method a series of steps either up or down are connected by a constant depth region followed by a series of steps in the other direction. In this method, as in the case of a trench or a sill, a domain with J regions will contain $J-1$ steps and boundaries. Each region has a specified depth and each boundary between region has a specified x location where the matching conditions must be applied(Fig. 2).

At each boundary, the matching conditions are applied and depend on whether the boundary is a step up or a step down. With the incident wave specified, a set of equations with $2(J-1)N+2(J-1)$ unknown coefficients is formed. In this study, we included the first evanescent mode, $N=1$.

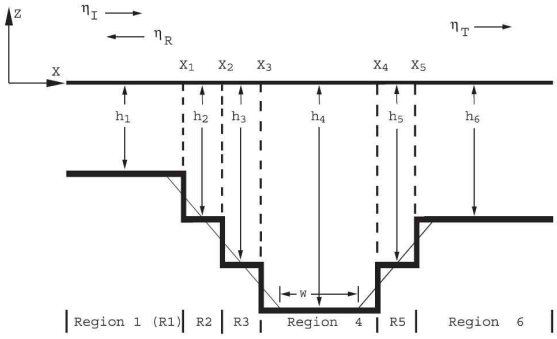

Fig. 2. Schematic sketch of an arbitrarily varying topography.

4. Results

4.1 Permeable shoal

Flaten and Rygg(1991) have examined the wave propagation over a single-layer porous shoal. The thickness of the shoal is described by the following equations(Fig. 3)

$$h = \begin{cases} h_0 & x < 0 \\ h_0 - b - b\sin(lx - \pi/2) & 0 < x < 0.5\lambda_s \\ h_0 - 2b & 0.5\lambda_s < x < W - 0.5\lambda_s \\ h_0 - b - b\sin(lx - \pi/2) & W - 0.5\lambda_s < x < W \\ h_0 & x > W \end{cases} \tag{26}$$

where b is the half height of the shoal crest, $l = 2\pi/\lambda_s$, W is the total length of the shoal, and λ and h_0 are the wave length and water depth, respectively, outside the shoal. In this study, $h_0 = 10m$, $b = 2m$, and $W = 6\lambda_s = 300m$ were used, and three different values of permeability were tested: $K = 0.0$, 1.0×10^{-8}, and $4.0 \times 10^{-8} m^2$.

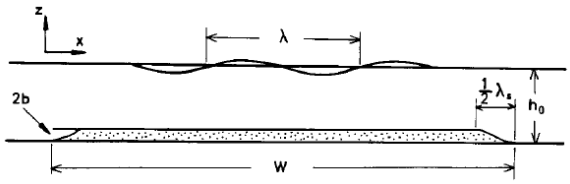

Fig. 3 Definition sketch of the porous shoal.

Fig. 4 compares the squared transmission coefficients behind the shoal calculated by the present method and the integral equation method of Flaten and Rygg(1991) as a function of λ/h_0. The agreement between the two methods is excellent, especially for the case of impermeable shoal of $K = 0.0m^2$. It should be noted that short waves are not influenced by the shoal if it is impermeable, see Fig. 4(a). However, as the permeability of the shoal increases, short

waves are more influenced than long waves, as shown in figs. 4(b) and 4(c). As the waves become very short, the influence of permeable bed upon surface water waves diminishes so that the wave transmission coefficient bounces back to increase.

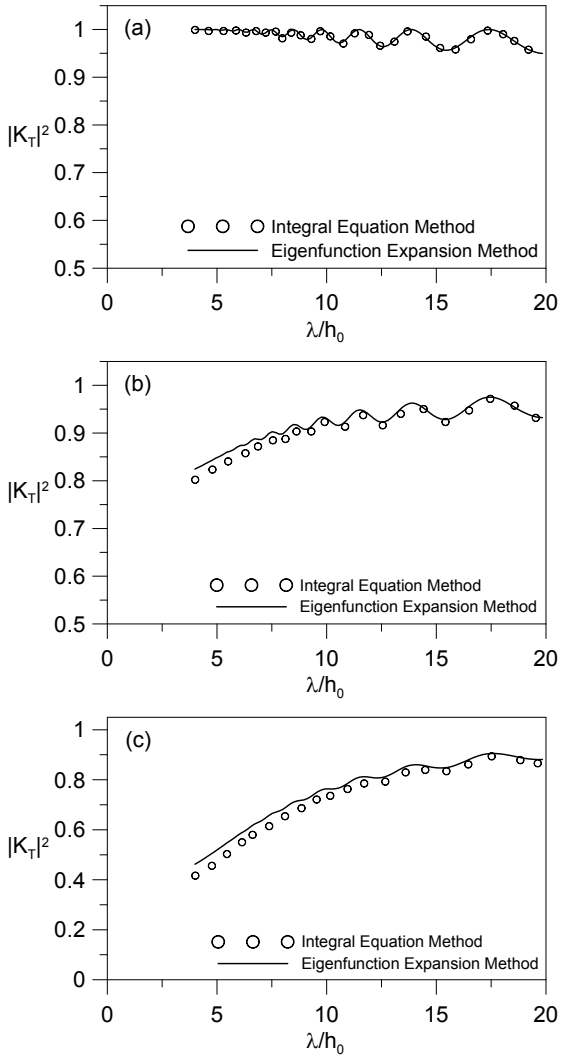

Fig. 4. Squared transmission coefficient for periodic waves over a shoal : (a) $K=0.0m^2$; (b) $K=1.0\times10^{-8}m^2$; (c) $K=4.0\times10^{-8}m^2$.

4.2 Permeable planar slope

We conducted numerical experiments for monochromatic waves propagating over a permeable planar slope each end of which was connected to a constant-depth impermeable region(Fig. 5). The experimental condition is similar to the case of submerged caisson breakwater armored with concrete blocks in front of the vertical wall. Tests for impermeable planar slope was first made by Booij(1983) who investigated the accuracy of the mild-slope equation. The water depths on the up- and down-wave sides of the slope are $h_1=0.6$ m and $h_2=0.2$ m, respectively, and the width of the sloping bottom b is varied so that the bottom slope varies. The permeability of the porous slope is fixed as $4.0\times10^{-8}m^2$. Tests were conducted with different wave frequencies of $f=0.35, 0.5, 0.75$ Hz to investigate wave reflections in a broad range of relative water depth.

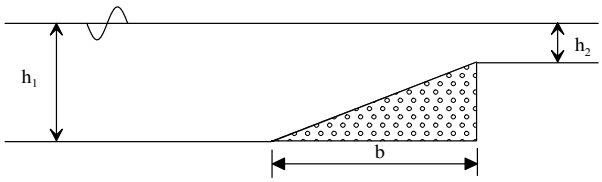

Fig. 5. Computational domain for numerical test of waves propagating over a porous planar slope.

Fig. 6 compares the squared transmission coefficients behind the porous slope calculated for several wave frequencies. This shows that the transmission became smaller for the longer slope width because the wave dissipation is significantly affected by the width of porous bed.. Moreover, as the wave frequency increased, the wave transmission decreased. This confirms the results for the permeable shoal.

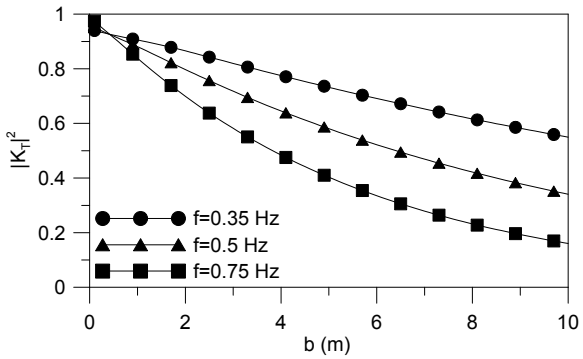

Fig. 6. Squared transmission coefficient for several wave frequency over porous planar slope.

Fig. 7 compares the reflection coefficient for several frequencies. As the wave frequency increased, the wave reflections decreased because the bottom was less felt in deeper waters. Also, with the higher wave frequency, there existed more numbers of resonant and non-resonant reflections with the slope-width variation. For the case of porous slope, the reflection coefficients were less than those of solid bottom. Moreover, the numbers of resonant reflection becomes smaller than those of solid bottom. These are

caused by the delay of wave speed and energy dissipation due to porous bottom. It should be noted that for the case of $f = 0.75$ Hz, the reflection coefficients over the porous slope is slightly higher than those of solid bottom for very long slope, but the difference is very small.

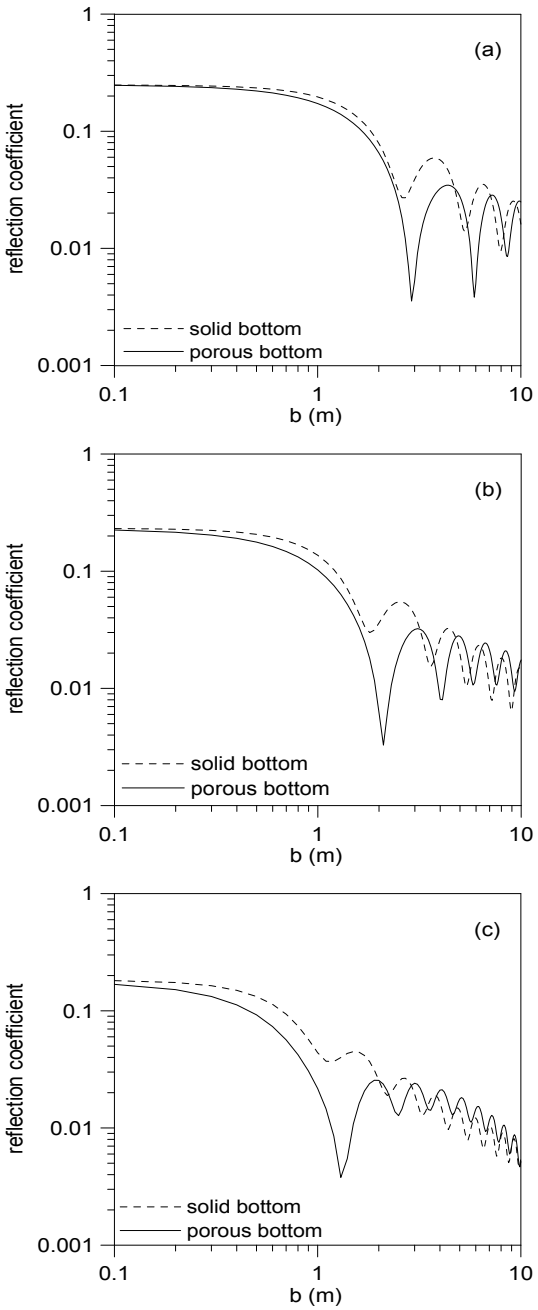

Fig. 7. Variation of reflection coefficients with width of a planar slope : (a) $f = 0.35$ Hz, (b) $f = 0.5$ Hz, (c) $f = 0.75$ Hz.

5. Conclusion

In this study, we applied the damping rate of waves propagating over a permeable seabed of finite depth to the eigenfunction expansion method which is able to include the evanescent mode as well as the propagating mode. First, the wave damping rate for a permeable bed was reviewed. Furthermore, the derived wave damping rate was applied in the eigenfunction expansion method to simulate a monochromatic wave propagating over a porous bed.

The results of numerical model including the dissipation term was compared with that of the integral equation method of Flaten and Rygg(1991) to show good agreement. The model was used to examine the wave transmission over the planar slope of permeable seabed. It was found that in general short waves are more influenced by the permeability of the planar slope than long waves. We also applied the numerical model to a porous planar slope. As a result, as the wave frequency increased, the wave transmission decrease. The reflection coefficients were also generally less than those of solid bottom. The delay of wave speed and energy dissipation made the numbers of resonant reflection smaller than those of solid bottom.

References

[1] Booij, N.(1983), A note on the accuracy of the mild-slope equation, Coastal Engineering, Vol. 7, pp. 191-203.

[2] Do, K. D. and K. D. Suh(2011), Wave damping over a multilayered, permeable seabed, Journal of Coastal Research, Vol. 27, No. 6, pp. 1183-1190.

[3] Flaten, G. and O. B. Rygg(1991), Dispersive shallow water waves over a porous sea bed, Coastal Engineering, Vol. 15, pp. 347-369.

[4] Guazzelli, E., V. Rey and M. Beizons(1992), Higher-order Bragg reflection of gravity surface waves by periodic beds, Journal of Fluid Mechanics, Vol. 245, pp. 301-317.

[5] Kirby, J. T. and R. A. Dalrymple(1983), Propagation of obliquely incident waves over a trench, Journal of Fluid Mechanics, Vol. 133, pp. 47-63.

[6] Liu, P. L. F. and R. A. Dalrymple(1984), The Damping of gravity water waves due to percolation, Coastal Engineering, Vol. 8, pp. 33-49.

[7] O'Hare, T. J. and A. G. Davies(1992), A new model for surface-wave propagation over undulating topography, Coastal Engineering, Vol. 18, pp. 251-266.

[8] Reid, R. O. and K. Kajiura(1957), On the damping of gravity waves over a permeable seabed, Transactions of American Geophysical Union Vol. 38, pp. 662-666.

[9] Takano, K.(1960), Effects d'un obstacle paralléllépipédique sur la propagation de la houle, Houille Blanche, Vol. 15, p. 247.

Received : 2012. 05. 15.
Revised : 2012. 06. 15. (1st)
2012. 06. 22. (2nd)
Accepted : 2012. 06. 25.